Carboxylic Acid-Functionalized Conductive Polypyrrole as a Bioactive Platform for Cell Adhesion

Joo-Woon Lee,*[,†,‡] Francisco Serna,[†,‡] Jonathan Nickels,[‡] and Christine E. Schmidt*[,§]

Department of Biomedical Engineering, The University of Texas at Austin, Austin, Texas 78712, and Texas Materials Institute, The University of Texas at Austin, Austin, Texas 78712

Received March 9, 2006; Revised Manuscript Received April 6, 2006

Electroactive polymers such as polypyrrole (PPy) are highly attractive for a number of biomedical applications, including their use as coatings for electrodes or neural probes and as scaffolds to induce tissue regeneration. Surface modification of these materials with biological moieties is desired to enhance the biomaterial−tissue interface and to promote desired tissue responses. Here, we present the synthesis and physicochemical characterization of poly(1-(2-carboxyethyl)pyrrole) (PPyCOOH), a PPy derivative that contains a chemical group that can be easily modified with biological moieties at the *N*-position of the polymer backbone. FTIR, XPS, and fluorescence microscopy were used to demonstrate the successful incorporation of carboxylic acid (−COOH) functionality into PPy materials, and a four-point probe analysis was used to demonstrate electrical conductivity in the semiconductor range. Human umbilical vascular endothelial cells (HUVECs) cultured on PPyCOOH films surface-modified with the cell-adhesive Arg-Gly-Asp (RGD) motif demonstrated improved attachment and spreading. Thus, PPyCOOH could be useful in developing PPy composites that contain a variety of biological molecules as bioactive conducting platforms for specific biomedical purposes.

Introduction

Conductive polymers based on polypyrrole (PPy) have been widely investigated for applications in fuel cells,[1a] electrochromic displays,[1a] biosensors,[1b] actuator components[1c] in microsurgical tools, and nerve repair conduits.[1d] Oxidized PPy can be electrochemically and chemically synthesized in the forms of films and powders, respectively, with the incorporation of negatively charged dopant ions. Upon doping, conductivity is generated by interchain hopping of π electrons, which can be influenced by factors such as polaron length, chain length, charge transfer to adjacent molecules, and conjugation length.[2] PPy conductivity and physical properties can be controlled by changing the dopant anions during syntheses.[2] PPy's versatility can be attributed to its good electrical conductivity, environmental stability to air and water, relative ease of synthesis through electrochemical and chemical routes, and the potential for copolymerization without compromising its electroactivity.[2] In addition, PPy has shown promise as a suitable substrate for the manipulation of cell growth and function and possesses excellent biocompatibility in vivo.[3] A need for conductive biomaterials exists because numerous tissues including bone,[4a] cartilage,[4b] skin,[4c] spinal nerves,[4d] and peripheral nerves[1d] respond favorably to electric fields.

From a separate standpoint, the development of bioactive materials able to improve cellular responses has been a dominant subject owing to the progress in understanding the molecular interactions that result in cell adhesion.[5] The Arg-Gly-Asp (RGD) motif is the minimal cell-recognizable sequence in many adhesive extracellular matrix proteins.[6] The immobilization of oligopeptides containing the RGD sequence on biomaterials is considered a valid strategy to provide cell-adhesive surfaces for use in biomedical applications.[7] Thus, tailoring PPy with functional groups to which a variety of biomolecules such as the RGD motif can be tethered will facilitate the building of biological structures on conducting surfaces.

Sanghvi et al. recently reported PPy surface functionalization using a unique peptide sequence ("T59") identified with the binding phage ("φT59"), selected by phage display and biopanning techniques.[8] The T59 peptide was successfully demonstrated as a bifunctional linker by conjugating a cell-adhesion-promoting sequence, Gly-Arg-Gly-Asp-Ser (GRGDS), at the *C*-terminus. However, the PPy-binding capability of T59 was significantly diminished in an acidic environment (pH < 4) because of the protonation of acidic Asp (D) residue of the T59 oligopeptide. Here we present an alternative approach to surface modification based on the covalent coupling of biological moieties through a peptide bond, which is typically more robust and less sensitive to pH. In this alternative chemical modification, a carboxylic acid-functionalized PPy, poly(1-(2-carboxyethyl)pyrrole) (PPyCOOH) demonstrates its promising potential as a bioactive platform for tissue engineering applications.

Experimental Section

1-(2-Cyanoethyl)pyrrole (Aldrich), potassium hydroxide (KOH, Fischer), sodium chloride (NaCl, Aldrich), iron(III) chloride ($FeCl_3$, Sigma), 1-ethyl-3-[3-(dimethylamino)propyl]carbodiimide (EDC, Fluka), *N*-hydroxysulfosuccinimide (NHSS, Sigma), 5-(aminoacetoamino)-fluorescein (Molecular Probes), GRGDSP peptide (Anaspec), human umbilical vascular endothelial cells (HUVECs, Cambrex), endothelial cell medium-ECM (Cambrex), and MTS reagent (Promega) were used as received; however, pyrrole (Sigma) monomer was purified by passing through a column of activated basic alumina prior to polymerization. Indium−tin oxide (ITO) conductive borosilicate glass slides with typical resistance of 30∼60 Ω (Delta Technologies, Ltd.) were sequentially ultrasonically cleaned in acetone, methanol, isopropyl alcohol, and DDI

* To whom correspondence should be addressed. E-mail: jwoonlee@mail.cm.utexas.edu (J.-W.L.); schmidt@che.utexas.edu (C.E.S.).

† These authors contributed equally to this work.

‡ Department of Biomedical Engineering.

§ Texas Materials Institute.

10.1021/bm060220q CCC: $33.50
Published on Web 05/03/2006

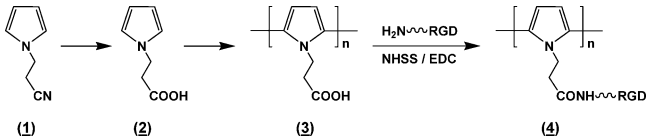

Figure 1. Synthetic scheme of carboxylic acid-functionalized conductive polypyrrole, poly(1-(2-carboxyethyl)pyrrole (PPyCOOH) (**3**), and the chemical conjugation with RGD peptide, RGD-grafted PPyCOOH (**4**).

water for 5 min each. Slides were then dipped in a 1.0 N NaOH solution for 30 min, washed with copious amounts of DDI water, and dried under vacuum.

Schematic chemical reactions for the synthesis of carboxylic acid-functionalized polypyrrole and the immobilization of a RGD peptide were presented in Figure 1.

Monomer Synthesis. Monomeric 1-(2-carboxyethyl)pyrrole (**2**) precursor was hydrolyzed from 1-(2-cyanoethyl)pyrrole (**1**) as described elsewhere.[9] Briefly, 12.5 g of 1-(2-cyanoethyl)pyrrole (**1**) was added to 60 mL of KOH (6.7 M). This mixture was refluxed under argon atmosphere until no more $NH_3(g)$ evolved. The reddish solution was acidified to pH 5 using 8 M HCl, and the product was then extracted with diethyl ether. The diethyl ether was evaporated, and the resulting crude product was twice recrystallized from boiling *n*-heptane to the white crystalline product (overall yield 69%). The NMR and IR spectra (not shown) confirmed the structure and were in agreement with the literature.[9]

Polymer Preparation. PPyCOOH Polymer films and powders were prepared both electrochemically and chemically, respectively. The chloride-doped PPyCOOH (**3**) (*or* PPy) films were electrochemically synthesized using a Bi-potentiostat (AFRDE5, Pine Instrument) in a three-electrode cell: a platinum (Pt) mesh served as the counter electrode, a saturated calomel electrode (SCE) served as the reference electrode, and an ITO slide served as the working electrode. The aqueous monomer solution (200 mL) containing 0.1 M 1-(2-carboxyethyl)pyrrole (**2**) (*or* pyrrole) and 0.1 M NaCl was purged with N_2 for 10 min to prevent oxidation of the monomer prior to polymerization. The films were deposited at an offset voltage of 720 mV onto the ITO electrode. The film thickness was controlled by integrating the passage of current.[8] The chloride-doped PPyCOOH (**3**) (or PPy) powders were chemically synthesized by oxidizing 14.4 mmol of 1-(2-carboxyethyl)-pyrrole (**2**) (or pyrrole) monomer into 100 mL of $FeCl_3$ (36.0 mmol) aqueous solution for 24 h at ambient temperature. The resulting black precipitate was vacuum-filtered and washed with copious amounts of DDI water until the washings were clear. The powder was then dried in a desiccator overnight and sieved to a diameter of 75~150 μm.

Surface Modification and Cell Adhesion. A cell-adhesive GRGD-SP was immobilized onto the surface of PPyCOOH (**3**) films in 10 mM PBS at pH 7.4 as follows. A solution of 173 μM EDC and 15 μM NHSS was reacted with the PPyCOOH film for 3 h at ambient temperature to activate the carboxylic acid groups on the surface in a stable intermediate form of *N*-sulfosuccinimidyl ester polypyrrole. GRGDSP peptide (1 mg/mL) was then chemically conjugated with the film surface for 4 h, leading to the formation of RGD-grafted PPyCOOH (**4**). To validate this coupling reaction in advance, the same procedure has been successfully conducted to attach a primary amine containing fluorescent molecule, 5-(aminoacetoamino) fluorescein ($\lambda_{Abs} = 491$ nm and $\lambda_{Em} = 515$ nm), to the PPyCOOH film and powder surfaces.

Cell adhesion studies have been qualitatively and quantitatively performed in the presence and absence of serum. HUVECs were seeded in 1.5 cm^2 wells with 1 mL of ECM media at a density of 30 000 cells/cm^2 and cultured for 6 h in 2% fetal bovine serum (FBS) onto RGD-grafted PPyCOOH (**4**) and a negative control PPy for the qualitative cell adhesion study. The colorimetric MTS cell proliferation assay was performed to quantify the extent of cell adhesion.[10] Cells were plated in the absence of serum and allowed to attach for 1 h. Surfaces were then rinsed three times by gently shearing 1 mL of 10 mM PBS over the film surface to remove unattached and loosely attached cells.[8] PBS was aspirated and a new medium containing 2% FBS and 20% MTS reagent was added to each well and allowed to incubate at 37 °C for 1, 2, and 3 h time points. Cell viability was measured by removing 100 μL of media from the wells and measuring the absorbance at 490 nm.

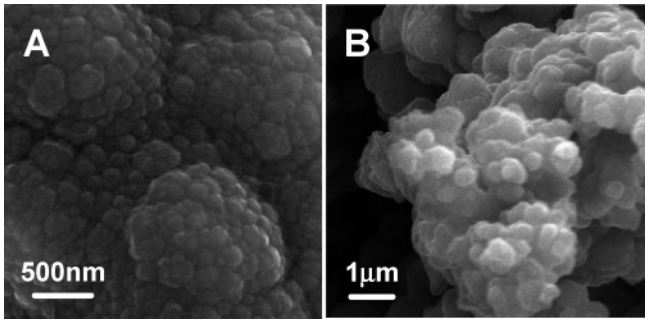

Figure 2. SEM images demonstrating the typical features of PPyCOOH films (A) and PPy powders (B). Similar morphologies are also observed for PPyCOOH powders and PPy films, respectively.

Polymer Characterization and Cell Viability. Polymer surface composition was determined using X-ray photoelectron spectroscopy (XPS) (PHI 5700, Physical Electronics), and bulk chemical characterization was carried out using FTIR (Infinity Gold, Thermo Mattson). The doping level was determined from the Cl/N ratio of high-resolution Cl(2p) and N(1s) core-level XPS spectra. Film thickness was measured using scanning electron microscopy (SEM) (LEO 1530) and a profilometer (Alpha Step 200, Tencor Instruments). Conductivity at ambient temperature was measured with a conventional four-point probe resistivity apparatus placed on the polymer films and the flat surfaces of pellets that were prepared by pressing the polymer powders at 18 000 psi. Morphology and qualitative cell adhesion analysis were performed using SEM and optical microscopy (Olympus IX-70), respectively.

The viability of HUVECs was assessed quantitatively based on the reduction of MTS (tetrazolium salt) to a colored formazan compound by viable cells in culture.[10] Metabolism in the viable cells produces a reducing equivalent, NADH, which passes its electron to an intermediate electron-transfer reagent that can reduce MTS into the aqueous, formazan product. The production of the product is proportional to the number of viable cells. Therefore, the absorbance of the colored formazan product was measured at 490 nm as a function of time with a fluorescence microplate reader (Synergy HT, Bio-Tek).

Results and Discussion

PPyCOOH and PPy (control) films and powders were synthesized as described in the Experimental Section and characterized to compare physical and chemical properties with the intention of selecting the most adequate surface for initial cell adhesion studies. Microscopic and spectroscopic characterization was carried out for both films and powders of PPyCOOH and PPy. The morphology of the polymers was investigated using SEM. Figure 2 presents the typical features of PPyCOOH films (A) and PPy powders (B). The cauliflower-like morphology of PPyCOOH films in Figure 2A is identical to that of typical PPy thin films[11a] electrodeposited on ITO slides, and the spherical feature of PPy aggregates in Figure 2B is also typically observed in PPyCOOH powders.[11b]

Table 1 shows the physical characteristics of PPyCOOH films and powders, along with PPy films and powders as a reference. The thickness of PPy films was measured from cross-sectional SEM images. The thickness of PPyCOOH films was determined using a profilometer because of the difficulty in delaminating the film for SEM imaging. The doping levels were calculated from the Cl/N ratios of high-resolution XPS. The relatively lower doping level of PPyCOOH compared with PPy

Table 1. Physical Properties of PPyCOOH and PPy Films and Powders

property sample		thickness (nm)	doping level[a] (%, Cl/N ratio)	conductivity (σ, S/m)
PPyCOOH	film	ca. 150	12.8	4.65×10^{-2}
	powder	n/a	4.9	2.83×10^{-2}
PPy	film	250−400	26.6	2.81×10^{2}
	powder	n/a	23.9	2.83×10^{2}

[a] From high-resolution XPS spectra.

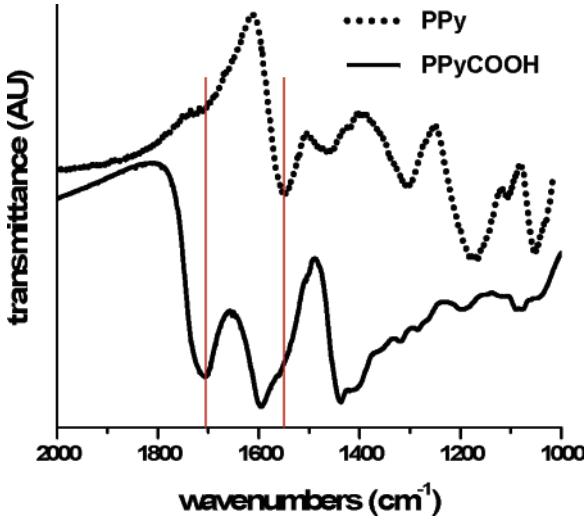

Figure 3. FTIR spectra of PPyCOOH and PPy powders. The strong band at 1703 cm^{-2} of PPyCOOH (solid line) confirmed the presence of carboxylic acid (−COOH) functionality in bulk. Note the vertical lines at 1703 and 1548 cm^{-1} represent the positions of ν_{COOH} and ν_{N-H}, respectively.

was believed to result from the rate of decrease in the polymerization associated with the carboxyethyl group substituted at the *N*-position of pyrrole. The electrical conductivity of PPyCOOH was measured to be on the order of 10^{-2} S/m, which is in the range (10^{2}∼10^{-6} S/m)[9b,12] of semiconductor materials such as silicon and germanium. The significant decrease in the conductivity in PPyCOOH as compared with PPy (10^{2} S/m) can be attributed to the disruption in planarity and the resulting disruption of the π-electron conjugation.[13] For tissue engineering and regenerative purposes, the semiconductor range of conductivity is sufficient;[14a,b] however, a layer-by-layer (LbL) composite[14c] consisting of PPyCOOH over PPy would allow both higher conductivity and a functionalized surface for biosensing applications as a bioactive electrode.

The presence of the carboxylic acid (−COOH) functionality in bulk was confirmed using FTIR. PPy and PPyCOOH powders were blended with anhydrous KBr and pressed into a pellet by a hydraulic press for analysis. The PPy FTIR spectrum (Figure 3, dashed line) shows a prominent strong band at 1548 cm^{-1} corresponding to the H−N stretching of the monomeric pyrrole unit of the backbone structure, whereas the spectrum of PPyCOOH (solid line) exhibits a characteristic band attributable to the carboxylic acid groups at 1703 cm^{-1} that is absent in the reference PPy, indicating the presence of carboxylic acid groups at the *N* positions of PPy.

To further verify the presence of carboxylic functionality at the surface, the chemical composition (in atomic %) of PPyCOOH was determined using XPS. No foreign element except C(1s), N(1s), O(1s), and Cl(2p) was detected in the survey spectra (not shown) from the films and powders. The high-resolution C(1s) region of XPS provides direct evidence

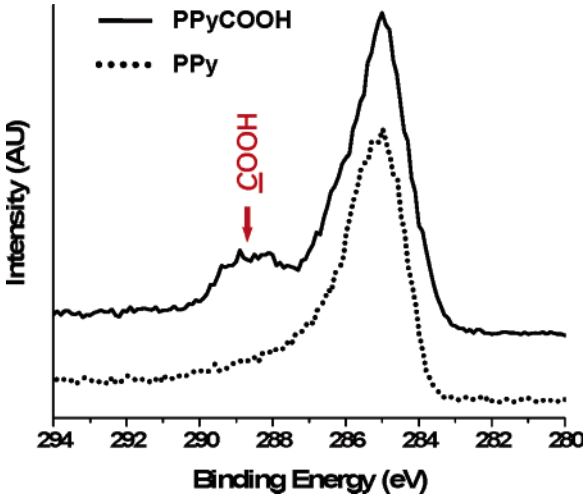

Figure 4. High-resolution XPS spectra relevant to C(1s) regions of PPyCOOH and PPy films, respectively. A characteristic peak of PPyCOOH (solid line) observed at 288.8 eV is assigned to carboxylic acid, −*C*OOH, functionality.

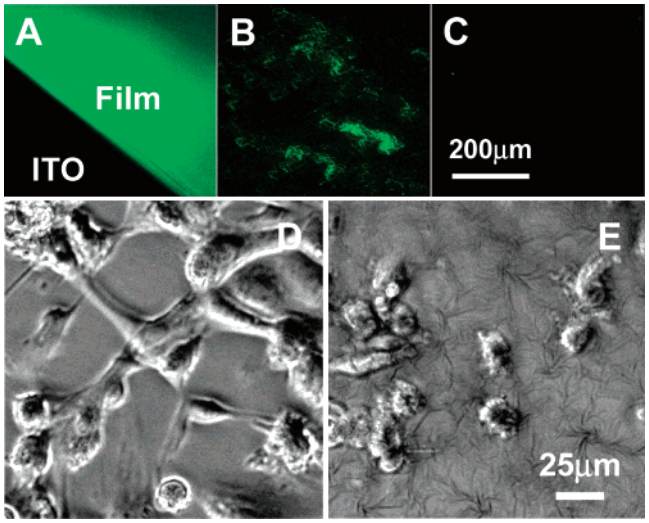

Figure 5. Typical fluorescent (top) and phase-contrast (bottom) images of the labeled PPyCOOH films (A) and powders (B), the control PPy films (C), cells (HUVECs) on the RGD-grafted PPyCOOH films (D), and on the control PPy films (E) cultured for 6 h at an initial density of 30 000 cells/cm^2. The coupling reaction to form a peptide bond between carboxylic acid (−COOH) of PPyCOOH and primary amine (H_2N−) functionalities was indirectly validated in the fluorescence images (A, B, and C) of 5-(aminoacetoamino) fluorescein as a model primary amine compound, supporting the RGD peptide conjugation onto the surface of PPyCOOH for cell adhesion (D and E).

for the presence of carboxylic acid groups at the surface of PPyCOOH films in Figure 4, where the binding energy of the C(1s) *C*−C/*C*−H_x component centered at 284.6 eV aligns with that of reference PPy for the comparison. The presence of carboxylic acid (−COOH) groups at the surface of PPyCOOH was readily detected by the appearance of a new C(1s) component centered at 288.8 eV.[15]

Surface modification of the −COOH of PPyCOOH into an amide (−NHCO−) via a peptide bond was confirmed by chemically conjugating a primary amine-containing fluorescein, 5-(aminoacetoamino) fluorescein. Fluorescent optical microscopy images in Figure 5, panels A and B, demonstrate the fluorescein immobilization onto the surface of PPyCOOH films and powders, respectively. Figure 5C shows the control PPy film subjected to the same surface treatment; however, there

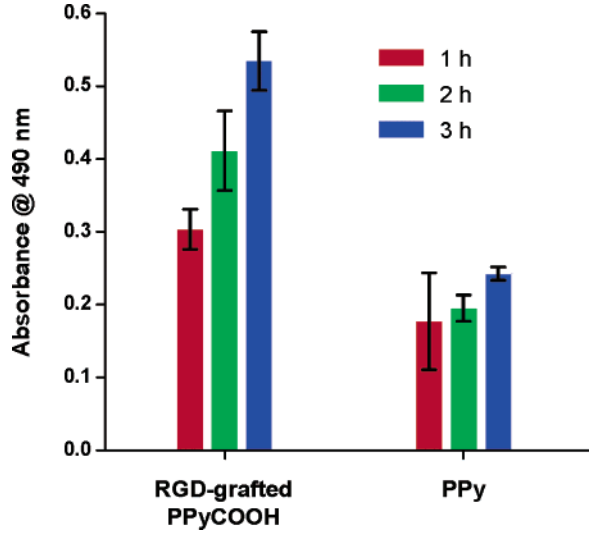

Figure 6. Cell (HUVEC) viability measured on the RGD-grafted PPyCOOH and the control PPy as a function of incubation time, using an MTS cell proliferation assay. For all samples $n = 2-5$, typically 5. Error bars represent the standard deviation (SD).

was no noticeable fluorescence. Both film and powder PPyCOOH successfully demonstrated covalent bonding between the carboxylic acid (−COOH) and primary amine (H_2N-) through formation of a peptide bond (−NHCO−). In subsequent cell adhesion studies, however, only film-type PPyCOOH and PPy were studied because of the convenience in handling sample specimens for cell culture analysis. The *N*-terminus of a model peptide (GRGDSP) that promotes cell adhesion was covalently conjugated to the −COOH of PPyCOOH film surfaces and followed by HUVEC cell seeding and culture for 6 h. Figure 5, panles D and E, presents the phase-contrast images to validate that cells attach and spread on the RGD-grafted PPyCOOH surfaces to a greater extent than on control PPy.

Cell quantification was also conducted to determine the extent of HUVEC adhesion on RGD-grafted PPyCOOH film surfaces, using the MTS cell assay.[10] The column data in Figure 6 represent the average absorbance at 490 nm of the formazan product derived from the reduction of MTS, and the error bars reflect the standard deviation (SD) at each incubation time point. The results indicate that the RGD-grafted PPyCOOH increased the viability of HUVECs by more than a factor of 2 compared with the control PPy. As an additional control, cell viability on pristine PPyCOOH after 3 h incubation was assayed and found not to be statistically different from the cell viability on PPy (absorbance = 0.27 for PPyCOOH and 0.25 for PPy, $n = 3$). This suggests that the conjugated RGD is the critical factor in promoting cell adhesion. The superior ability of the RGD-grafted surface to promote cell proliferation validates the utility of the carboxylic acid-functionalized polypyrrole as a bioactive platform. This platform can be further optimized for tissue engineering and bioelectric applications by tethering growth factors and other biologically important moieties to the polypyrrole surface.

Conclusion

An acid-functionalized PPy substituted at the *N*-position, poly(1-(2-carboxyethyl)pyrrole) denoted as PPyCOOH, was demonstrated as a bioactive platform for surface modification and cell attachment. PPyCOOH films were prepared by electrochemical polymerization of 1-(2-carboxyethyl)pyrrole monomer that was synthesized from 1-(2-cyanoethyl)pyrrole. RGD-grafted PPyCOOH was tailored by chemically conjugating an RGD-containing peptide, GRGDSP, onto the surface of PPyCOOH. HUVECs seeded on RGD-grafted PPyCOOH surfaces demonstrate an improved ability to attach to the surface and spread. Further studies are currently underway to fabricate PPyCOOH with higher conductivity using an electrochemical layer-by-layer (LbL) deposition technique, and to synthesize and characterize monomeric pyrrole precursors that allow the introduction of biological molecules on the surface of conductive PPy derivatives.

Acknowledgment. The authors thank Prof. J. Mike White for conductivity measurement with a 4-point probe resistivity apparatus. This work was supported by the Gillson Longenbaugh Foundation, the National Institute of Health (R01EB004529), the National Science Foundation Graduate Fellowship to F.S. and, for support of the FTIR, the Center for Nano and Molecular Sciences and Technology.

References and Notes

(1) (a) Pruneanu, S.; Resel, R.; Leising, G.; Brie, M.; Graupner, W.; Oniciu, L. *Mater. Chem. Phys.* **1997**, *48*, 240. (b) Brahim, S.; Guiseppi-Elie, A. *Electroanalysis* **2005**, *17*, 556. (c) Otero, T. F.; Sansiñena, J. M. *Bioelectrochem. Bioenerg.* **1997**, *42*, 117. (d) Schmidt, C. E.; Shastri, V. R.; Vacanti, J. P.; Langer, R. *Proc. Natl. Acad. Sci. U.S.A.* **1997**, *94*, 8948.

(2) (a) Skotheim, T. A.; Elsenbaumer, R.; Reynolds, J. *Handbook of Conducting Polymers*; Marcel Dekker: NewYork, 1998. (b) Kiess, H. G. *Conjugated Conducting Polymers*; Springer: Berlin, 1992.

(3) (a) George, P. M.; Lyckman, A. W.; LaVan, D. A.; Hegde, A.; Leung, Y.; Avasare, R.; Testa, C.; Alexander, P. M.; Langer, R.; Sur, M. *Biomaterials* **2005**, *26*, 3511. (b) Cui, X.; Lee, V. A.; Raphael, Y.; Wiler, J. A.; Hetke, J. E.; Anderson, D. J.; Martin, D. C. *J. Biomed. Mater. Res.* **2001**, *56*, 261. (c) Chen, S. J.; Wang, D. Y.; Yuan, C. W.; Wang, X. D.; Zhang, P. Y.; Gu, X. S. *J. Mater. Sci. Lett.* **2000**, *19*, 2157.

(4) (a) Spadaro, J. A. *Bioelecromagnetics* **1997**, *18*, 193. (b) Takei, J.; Akai, M. *Arch. Orthop. Trauma Surg.* **1993**, *112* (4), 159. (c) Goldman, R.; Solomon, P. *Bioelectromagnetics* **1996**, *17* (6), 450. (d) Politis, M. J.; Zanakis, M. F. *Neurosurgery* **1989**, *25* (1), 71.

(5) De Giglio, E.; Sabbatini, L.; Colucci, S.; Zambonin, G. *J. Biomater. Sci. Polym. Ed.* **2000**, *11*, 1073.

(6) (a) Pierschbacher, M. D.; Ruoslahti, E. *Nature* **1984**, *309*, 30. (b) Ruoslahti, E.; Pierschbacher, M. D. *Science* **1987**, *238*, 491.

(7) (a) Cook, A. D.; Hrkach, J. S.; Gao, N. N.; Johnson, I. M.; Pajvani, U. B.; Cannizzaro, S. M.; Langer, R. *J. Biomed. Mater. Res.* **1997**, *35*, 513. (b) Bearinger, J. P.; Castner, D. G.; Healy, K. E. *J. Biomater. Sci. Polym. Ed.* **1998**, *9*, 629.

(8) Sanghvi, A. B.; Miller, K. P−H; Belcher, A. M.; Schmidt, C. E. *Nature Mater.* **2005**, *4*, 496.

(9) (a) Azioune, A.; Slimane, A. B.; Hamou, L. A.; Pleuvy, A.; Chehimi, M. M.; Perruchot, C.; Armes, S. P. *Langmuir* **2004**, *20*, 3350. (b) Maeda, S.; Corradi, R.; Armes, S. P. *Macromolecules* **1995**, *28*, 2905.

(10) Barltrop, J. A.; Owen, T. C.; Cory, A. H.; Cory, J. G. *Bioorg. Med. Chem. Lett.* **1991**, *1*, 611.

(11) (a) De Giglio, E.; Guascito, M. R.; Sabbatini, L.; Zambonin, G. *Biomaterials* **2001**, *22*, 2609. (b) Ruangchuay, L.; Sirivat, A.; Schwank, J. *React. Funct. Polym.* **2004**, *61*, 11.

(12) Kiani, M. S.; Mitchell, G. R. *Synth. Met.* **1992**, *46*, 293.

(13) Diaz, A. F.; Castillo, J. A.; Logan, J. A.; Lee, W. Y. *J. Electroanal. Chem.* **1981**, *129*, 115.

(14) (a) Rivers, T. J.; Hudson, T. W.; Schmidt, C. E. *Adv. Funct. Mater.* **2002**, *12*, 33. (b) Wong, J. Y.; Labger, R.; Ingber, D. E. *Proc. Natl. Acad. Sci. U.S.A.* **1994**, *91*, 3201. (c) Collier, J. H.; Camp, J. P.; Hudson, T. W.; Schmidt, C. E. *J. Biomed. Mater. Res.* **2000**, *50*, 574.

(15) Azioune, A.; Siroti, F.; Tanguy, J.; Jouini, M.; Chehimi, M. M.; Miksa, B.; Slomkowski, S. *Electrochim. Acta* **2005**, *50*, 1661.

BM060220Q